New analytical calculations of the resonance modes in lens-shaped cavities: applications to the calculations of the energy levels and electronic wavefunctions in quantum dots

2003 J. Phys. A: Math. Gen. 36 11677

(http://iopscience.iop.org/0305-4470/36/46/010)

INSTITUTE OF PHYSICS PUBLISHING JOURNAL OF PHYSICS A: MATHEMATICAL AND GENERAL

J. Phys. A: Math. Gen. **36** (2003) 11677–11686 PII: S0305-4470(03)65566-6

New analytical calculations of the resonance modes in lens-shaped cavities: applications to the calculations of the energy levels and electronic wavefunctions in quantum dots

J Even and S Loualiche

Laboratoire d'Etude des Nanostructures à Semiconducteurs, INSA de Rennes, 20 Avenue des Buttes de Coesmes, CS 14315, F34043 Rennes Cedex, France

E-mail: jacky.even@insa-rennes.fr

Received 2 July 2003
Published 5 November 2003
Online at stacks.iop.org/JPhysA/36/11677

Abstract

The problem of the energy levels and electronic wavefunctions in quantum dots is studied in the parabolic coordinates system. A conventional effective mass Hamiltonian is written. For an infinite potential barrier, it is related to the more general problem of finding the resonance modes in a cavity. The problem is found to be separable for a biconvex-shaped cavity or quantum dot with an infinite potential barrier. This first shape of quantum dot corresponds to the intersection of two orthogonal confocal parabolas. Then plano-convex lens-shaped cavities or quantum dots are studied. This problem is no more separable in the parabolic coordinates but using symmetry properties, we show that the exact solutions of the problem are simple combinations of the previous solutions. The same approach is used for spherical coordinates and hemispherical quantum dots. It is finally shown that convex lens-shaped quantum dots give a good description of self-organized InAs quantum dots grown on InP.

PACS numbers: 71.15.m, 73.20.Dx

1. Introduction

Recent research developments were devoted to quantum dots semiconductor heterostructures. Their properties improve optoelectronic device performances as compared to semiconductor quantum wells [1–3]. The theoretical study of the electronic properties of quantum dots (QDs) can be performed with various theoretical schemes such as first-principles calculations, semi-empirical calculations (pseudopotential, tight binding) effective-mass or multiband $k \cdot p$ approximations. One-band effective mass models have proved to be very useful in many cases

for QDs grown either on GaAs or InP substrates [4–8]. Effective mass calculations for highly symmetric shapes (spherical QDs, cylindrical QDs) give first indications about the influence of three-dimensional (3D) quantum confinement [1, 2]. Ellipsoidal [9] or elliptic cylindrical QDs [10] have also been studied. There is however a lack of simple model in the case of asymmetric quantum dots. Indeed in many cases pyramids, truncated pyramids or lenses provide better spatial descriptions of the quantum dot geometries than spheres, ellipsoids or even parallelepipeds. Lens-shaped quantum dots have been simulated by various methods, such as finite differences, finite elements [7], transfer matrix [11] or conformal mapping associated with Rayleigh–Schrödinger perturbation theory [12]. However, up to now, no analytical solutions have been proposed. In this work for an infinite potential barrier, we use parabolic coordinates to get separable solutions related to solutions of Laplace and Helmholtz equations [13–16]. We show that various cavities or quantum dots shapes may be studied with parabolic coordinates using analytical solutions. These solutions are either confluent hypergeometric functions of the first kind or in some particular cases Bessel functions of the first kind. They may be easily computed using integral representations [15] or commercial mathematical packages [17]. Self-organized InAs quantum dots grown on InP with a lens shape are then conveniently studied [7, 18, 19]. A comparison to hemispherical quantum dots is also performed.

2. Biconvex-shaped quantum dot

2.1. Geometrical description of the dot

The parabolic set of unit less coordinates (u, v, θ) $(0 \leqslant u \leqslant \infty, 0 \leqslant v \leqslant \infty$ and $0 \leqslant \theta \leqslant 2\pi)$ is defined by a transformation of Cartesian coordinates :

$$x = auv\cos(\theta) \qquad y = auv\sin(\theta) \qquad z = a(u^2 - v^2)/2.$$

Figure 1(a) is a projection of the coordinate surfaces on the (y, z) plane. A particular volume is represented by the boundaries which are two parabolas $(u = U_0)$ and $(v = V_0)$ rotated around the z axis $(0 \leqslant \theta \leqslant 2\pi)$. In the particular case where $U_0 = V_0 = 1$, the surfaces are orthogonal confocal coordinate surfaces, which can be associated with the physical boundaries of a disc-shaped dot (or a kind of 'flying saucer') (figure 1(b)). The dot is represented by its height $T = a$ and its diameter $D = 2a$. The volume of the disc is equal to $\pi a^3/2$. Figure 1(c) corresponds to half the volume of the same disc $(\pi a^3/4)$ and to a lens-like shape with height $T = a/2$ and diameter $D = 2a$. The symmetry group is $D_{\infty h}$ in the first case and only $C_{\infty v}$ in the last case. In the last case, a symmetry plane perpendicular to the rotation axis is removed. The $D_{\infty h}$ is the direct product of $C_{\infty v}$ and C_i: the solutions in the second case may be deduced from the solutions in the first case. When electronic properties are considered [4–6], the quantum number n coming from the rotational symmetry dependence of the solution $(e^{in\theta})$ is used. It is usually associated with the labels S $(n = 0)$, P $(n = 1)$, D $(n = 2)$ ... for the $C_{\infty v}$ or $D_{\infty h}$ groups.

2.2. Effective mass Hamiltonian

In order to construct the conventional effective mass Hamiltonian, the usual symmetrization of the expression $\frac{\vec{p}^2}{2m(\vec{r})}$ yields $\hat{H} = \frac{1}{2}\hat{p}\frac{1}{m(\vec{r})}\hat{p} + V(\vec{r})$ with $\hat{p} = -i\hbar\vec{\nabla}$ [4, 17]. The parabolic

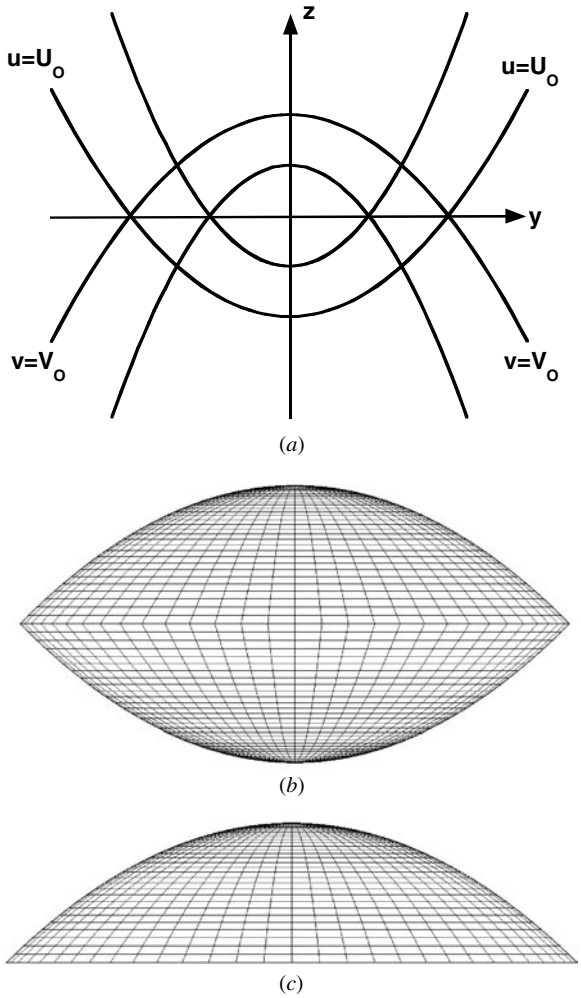

Figure 1. (*a*) Projection of the parabolic coordinate surfaces in the (y, z) plane. A particular volume is obtained by the boundaries which are two parabolas ($u = U_0$) and ($v = V_0$) rotated around the z axis ($0 \leqslant \theta \leqslant 2\pi$). If two orthogonal confocal parabolas are used ($U_0 = V_0$) a symmetrical disc-shaped volume is obtained (figure 1(*b*)). (*b*) Disc-shaped quantum dot obtained by the intersection of two orthogonal confocal parabolas (projection in the (y, z) plane). A mesh is used for drawing the external surface. (*c*) Lens-shaped quantum dot obtained by taking half the volume ($z > 0$) of the disc-shaped quantum dot (figure 1(*b*)). A mesh is used for drawing the external surface.

metric is defined by three coefficients: $h_{11} = h_{22} = a(u^2 + v^2)^{1/2}$ and $h_{33} = auv$ [13]. The gradient vector is

$$\vec{\nabla}\Psi = \begin{vmatrix} \dfrac{1}{a(u^2+v^2)^{1/2}}\dfrac{\partial\Psi}{\partial u} \\ \dfrac{1}{a(u^2+v^2)^{1/2}}\dfrac{\partial\Psi}{\partial v} \\ \dfrac{1}{auv}\dfrac{\partial\Psi}{\partial\vartheta}. \end{vmatrix}$$

When considering the geometry of the quantum dot (figure 1), the effective mass and the potential depend on (u, v) but not on θ (in the case of a finite potential barrier).

$$H = \frac{-\hbar^2}{2}\vec{\nabla}\frac{1}{m(\vec{r})}\vec{\nabla} + V(\vec{r}) = -\frac{\hbar^2}{2a^2(u^2+v^2)}\left[\frac{1}{u}\frac{\partial}{\partial u}\frac{u}{m_{(u,v)}}\frac{\partial}{\partial u} + \frac{\partial}{\partial v}\frac{v}{m_{(u,v)}}\frac{\partial}{\partial v}\right] - \frac{\hbar^2}{2a^2u^2v^2m_{(u,v)}}\frac{\partial^2}{\partial\theta^2} + V(u, v).$$

The Hamiltonian is separable in (u, v) and θ and $\Psi(u, v, \theta) = \chi(u, v)\,\mathrm{e}^{\mathrm{i}n\theta}$ are general solutions of the problem ($C_{\infty v}$ or $D_{\infty h}$ symmetry groups). No further separation is possible because of the complex dependence of the potential $V(u, v)$ associated with the boundary conditions.

2.3. Analytical solutions

In the case of an infinite potential barrier, $V(u, v)$ is set equal to zero and the effective mass is associated with the inner dot mass and is constant. The Schrödinger equation in this case is the Helmholtz equation [13]. We will consider here the problem of the quantum disc explicitly although this problem is in fact related to the more general problem of the resonance modes in a cavity. This is of interest for various problems in mechanics, acoustics or electromagnetism [14]. The Hamiltonian is separable in u, v and θ coordinates and the wavefunction is a product of functions of independent variables $\Psi(u, v, \theta) = f(u)g(v)\,\mathrm{e}^{\mathrm{i}n\theta}$. To simplify the analysis, energy variables are chosen to avoid problems related to the physical units: $E = E_\mathrm{r}/E_\infty$ where $E_\infty = \frac{\hbar^2}{2mT^2}$, E is the dimensionless energy and E_r is the real energy. The f and g functions are solutions of two coupled differential equations with a separation constant C:

$$u^2\frac{\mathrm{d}^2 f}{\mathrm{d}u^2} + u\frac{\mathrm{d}f}{\mathrm{d}u} + (Eu^4 - Cu^2 - n^2)f = 0$$

and

$$v^2\frac{\mathrm{d}^2 g}{\mathrm{d}v^2} + v\frac{\mathrm{d}g}{\mathrm{d}v} + (Ev^4 + Cv^2 - n^2)g = 0.$$

Solutions of these equations may be deduced from the literature [15], they include confluent hypergeometric functions ϕ:

$$f(u) = NF(u, C, E, n) = N\,\mathrm{e}^{-\mathrm{i}\sqrt{E}u^2/2}(\mathrm{i}\sqrt{E}u^2)^{n/2}\phi\left(\frac{-\mathrm{i}C}{4\sqrt{E}} + \frac{n+1}{2}, n+1, \mathrm{i}\sqrt{E}u^2\right)$$

$g(v) = NF(v, -C, E, n)$ where N is a normalization constant.

The boundary conditions are then $F(1, C, E, n) = 0$ and $F(1, -C, E, n) = 0$.

If we consider first the case $C = 0$, the two conditions reduce to a single condition $F(1, 0, E, n) = 0$. More, the solutions of the problem contain simple Bessel functions of complex variable z using the expression:

$$J_{n/2}(z) = \frac{\mathrm{e}^{-\mathrm{i}z}}{\Gamma\left(\frac{n}{2}+1\right)}\left(\frac{z}{2}\right)^{n/2}\phi\left(\frac{n+1}{2}, n+1, \mathrm{i}2z\right).$$

The solutions correspond to the zeros of $J_{n/2}(\sqrt{E}/2)$. Figure 2 is a representation of the lowest energy electronic wavefunctions for $n = 0$, $1\mathrm{S_e}$ and $n = 1$, $1\mathrm{P_e}$. The energies are respectively $E = 23.1$ and $E = 39.5$ in reduced energy units. It is important to note that these functions are even with respect to the plane symmetry $z \to -z$. This is a property common to all the solutions with $C = 0$. Indeed, the $z = 0$ surface is defined by $u = v$. Odd solutions should then vanish for any value of $u = v$ between 0 and 1. This condition cannot be fulfilled by the product of Bessel functions.

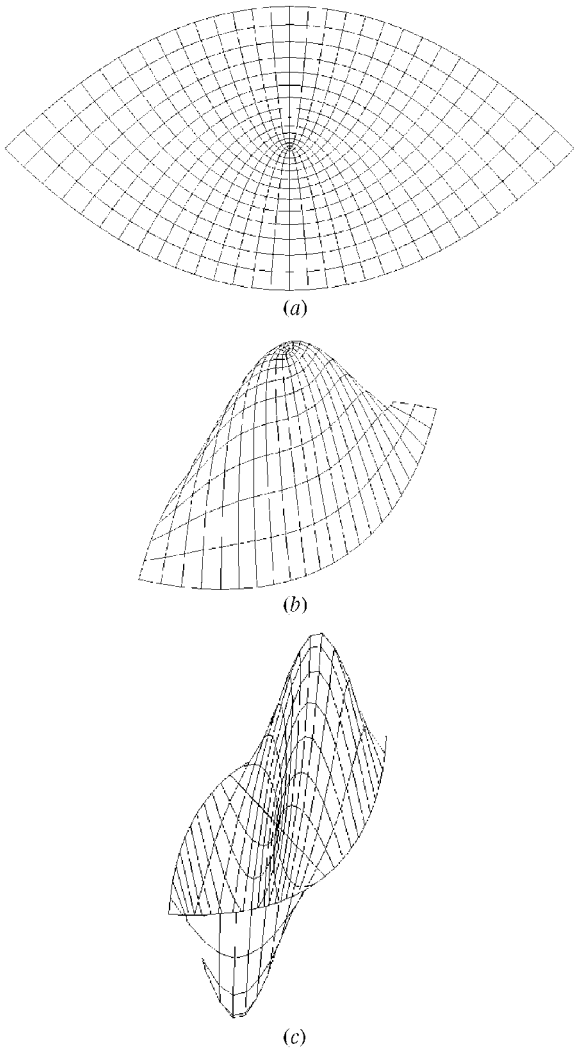

Figure 2. (*a*) Representation of the (u, v) mesh used for drawing the electronic wavefunctions (projection in the (y, z) plane). The surface is limited by the external boundary of the quantum disc. (*b*) Cross section of the fundamental state $1S_e$ wavefunction ((y, z) plane). A vertical scale is added and corresponds to the wavefunction amplitude. The separation constant C is equal to 0. (*c*) Cross section of the first excited state $1P_e$ wavefunction ((y, z) plane). A vertical scale is added and corresponds to the wavefunction amplitude. The separation constant C is equal to 0.

We consider now the case $C \neq 0$. The solutions correspond to putting $\phi\left(\frac{-iC}{4\sqrt{E}} + \frac{n+1}{2}, n+1, i\sqrt{E}\right)$ and $\phi\left(\frac{iC}{4\sqrt{E}} + \frac{n+1}{2}, n+1, i\sqrt{E}\right)$ simultaneously equal to zero. The numerical solution is then obtained by finding in the (C, E) plane, the intersection of the $E(C)$ curves corresponding to the minima. Figure 3 is a representation (limited to $C \geqslant 0$) of this procedure in the case $n = 0$. The lowest energy corresponds to $E = 62.0$ and $C = 13.5$. The same energy would have been obtained by considering $C = -13.5$. It means that all the solutions with $C \neq 0$ are twice degenerate. Figures 4(*a*) and (*b*) are representations of the two wavefunctions $\chi(u, v) = F(u, C, E, 0)^* F(v, -C, E, 0)$ and $\chi(u, v) = F(u, -C, E, 0)^* F(v, C, E, 0)$ corresponding to $E = 62.0$ and $C = 13.5$.

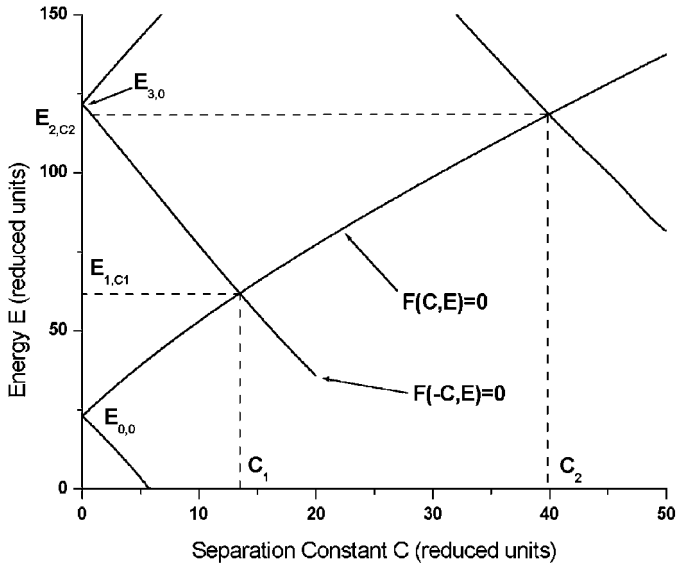

Figure 3. Representation of the $E(C)$ curves for $n = 0$ and limited to $C \geqslant 0$ (C is the separation constant and E is the energy). The eigenvalues are obtained by the intersections of two $E(C)$ curves. The ground-state $E_{0,0}$ corresponds to the intersection $E = 23.1$ and $C = 0$. Two states with $C \neq 0$ are obtained by the intersections of the $E(C)$ curves: $E_{1,C1} = 62.0$ with $C1 = 13.5$ and $E_{2,C2} = 118.6$ with $C2 = 40.0$. The next state is $E_{3,0} = 121.9$.

The constant C is related to the symmetries of the wavefunctions. The quantum number n is associated, in the case $n \neq 0$, with the breaking of the rotational symmetry around the z axis. In the same way, in the case $C \neq 0$, the plane symmetry $z \to -z$ is broken (figures 4(a) and (b)). It is however possible to classify the wavefunctions according to the IR of the $D_{\infty h}$ symmetry group by taking into account combinations of the degenerate solutions (figures 4(c) and (d)):

$$\chi(u, v) = F(u, C, E, 0)^* F(v, -C, E, 0) \pm F(u, -C, E, 0)^* F(v, C, E, 0).$$

The plus sign corresponds to the even $2S_e$ state (figure 4(c)) while the minus sign corresponds to the odd $1S_0$ state (figure 4(d)). These analytical solutions are no more separable solutions of the Schrödinger (Helmholtz) equation but provide a better description of the problem from the symmetry point of view.

3. Lens-shaped quantum dot

3.1. Analytical solutions

We will now consider the lens-shaped quantum dots (plano-convex lens) which correspond to half the volume of the previous geometrical object. The problem is not separable in the parabolic coordinates for the lens-shaped quantum dots because the boundary conditions on the horizontal plane ($z = 0$) strongly mix both coordinates ($u = v$). In relation to the infinite potential barrier now existing on the $z = 0$ plane, it is however straightforward to deduce that the solutions of this problem are the odd solutions of the previous one. The reduction of the thickness T by a factor of 2 has an important effect on the energy E_∞ which is increased by a

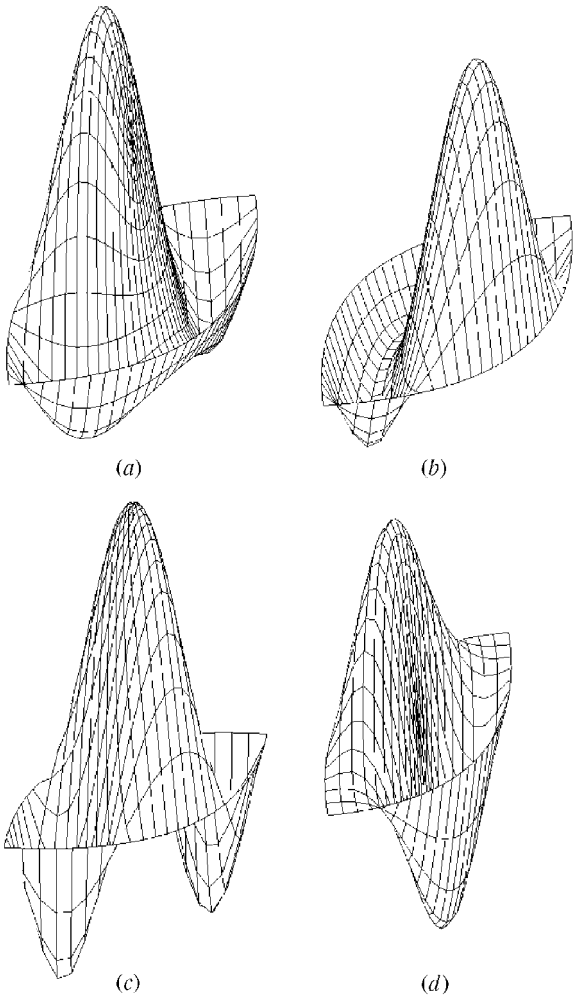

Figure 4. (*a*), (*b*) Cross sections of the two degenerate wavefunctions with $E_{1,C1} = 62.0$ ($C1 = 13.5$) in the (y), (z) plane ($n = 0$). A vertical scale is added and corresponds to the wavefunction amplitude. (*c*), (*d*) Cross sections of the even $2S_e$ and odd $1S_0$ wavefunctions which are combinations of the degenerate wavefunctions with $E_{1,C1} = 62.0$ ($C1 = 13.5$) ($n = 0$). A vertical scale is added and corresponds to the wavefunction amplitude.

factor of 4 $\left(E_\infty = \frac{\hbar^2}{2mT^2}\right)$. For the 1S ground state (former $1S_0$ state), we find then $E = 15.5$ and $C = 13.5$. The first excited state is the 1P state with $E = 21.9$ and $C = 21.7$. In order of increasing reduced energies, the next two states are the 1D ($n = 2$, $E = 29.0$ and $C = 29.7$) and 2S ($n = 0$, $E = 29.6$ and $C = 40.0$) states. The confined energies E_r *in the lens are higher than the ones in the disc.*

3.2. Comparison to other geometrical objects with analytical solutions

It is important to make a comparison to the case of the quantum well for two reasons. First, quantum wells are now widely used for optoelectronic devices [20] and quantum dots may offer improved performances for these applications [1–3]. Second, quantum wells correspond

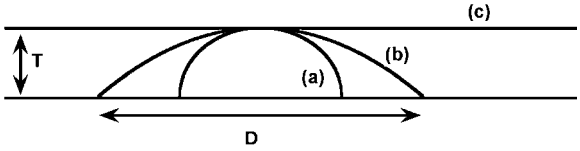

Figure 5. Cross sections ((y, z) plane) of an hemispherical quantum dot (a), a lens-shaped quantum dot (b) and a quantum well (c) with the same height T. D is the diameter of the lens-shaped quantum dot.

to a quantum confinement along only the z direction and may be considered as a limit where the diameter D tends to infinity (figure 5). For the infinite potential barrier case, the energy levels in the quantum wells with equivalent thickness to the quantum dot are quantified along z by the relation $E = (n\pi)^2$ where $n = 1, 2, 3, \ldots$ [20]. These energies correspond the edge of two-dimensional densities of states associated with the free motion in the (x, y) plane. The ground-state energy of the quantum well is equal to π^2. For the lens-shaped quantum dot, the energy is of the ground state is equal to $E = 15.5$. The increase from a value of π^2 for the quantum well to 15.5 for the quantum dots may be attributed to the quantum confinement in the (x, y) plane. It should be pointed out that there is a plane symmetry $z \rightarrow -z$ in the case of the quantum well but not for the lens-shaped quantum well. We may therefore predict that the behaviour of the two systems will be different with respect to a physical effect with vectorial symmetry along the z axis. This is the case of the quantum confined Stark effect (QCSE) where an applied field along z axis induces an energy level shift and modifies the matrix element of the optical absorption. A quadratic dependence of the ground-state energy shift is found in a quantum well in the case of the QCSE, where for the reason of symmetry, the linear term vanishes [20]. In comparison, a linear (stronger) dependence is theoretically expected for the lens-shaped quantum dots.

The case of the hemispherical quantum dot may also be analysed for comparison purposes (figure 5). The volume of this dot $2\pi T^3/3$ is smaller than the volume of the lens-shaped dot $2\pi T^3$ for the same height. Additional confinement may be expected in the horizontal plane in the hemispherical case. In order to obtain the analytical solutions for the hemispherical quantum dot problem, we may employ the same method as in sections 2 and 3.1. The analytical solutions for the spherical quantum dots are fully separable in the spherical coordinates, the electronic wavefunctions are then simple products of spherical harmonics (with quantum numbers ℓ and m) and radial Bessel functions of half integral order ($\ell = 1/2$) vanishing on the boundary $r = R$ (where R is the radius of the sphere) [1, 15]. The analytical solutions for the hemispherical quantum dot are the odd solutions of the spherical case when the plane symmetry $z \rightarrow -z$ is considered. The electronic ground state for the hemispherical quantum dot is defined by the spherical harmonic with $\ell = 1$, $m = 0$ and the first zero of the Bessel function with order equal to $3/2$. The ground-state reduced energy is $E = 20.2$ for a radius equal to the thickness of the quantum well and the lens-shaped quantum dot. The first excited state is degenerated (spherical harmonics with $\ell = 2$, $m = \pm 1$) with energy equal to $E = 33.2$, larger than the excited state energy of the lens-shaped dot $E = 21.9$ (section 3.1). For quantum objects of thickness T, the more the surface in the (x, y) plane is reduced, the more the confinement is increased.

3.3. Application in the case of InAs quantum dots grown on InP

An example of a lens-shaped geometry may be found for InAs quantum dots grown on InP [19]. These quantum dots are used for laser applications at the telecommunication wavelength of

1.55 μm [21] and present superior performances than devices realized on quantum wells [22]. For InAs quantum dots grown on InP (100) substrate the diameter and height are respectively equal to about 40 nm and 8 nm [19]. They can be well described by the geometry imposed by the parabolic coordinates (figure 1(a)) where the ratio between diameter and height is equal to 4. In addition, the facets of the dots show a tilt angle close to the value of 45° (figure 1(c)). Photoluminescence spectroscopy was used to study the optical transitions in these dots [7]. A ground-state optical transition energy of about 650 meV (or $E = 1092$ in reduced units) was measured at room temperature. Taking into account that the fundamental energy gap of the strained InAs material is $E = 722$ at room temperature [7], we deduce that the effect of quantum confinement on both the electrons and holes is equal to $E = 370$. The transition energy is calculated in our model by multiplying 15.5 by $1/\mu$ where μ is the reduced electron–hole mass. μ is then found equal to 0.042 which is in reasonable agreement with the effective masses usually used [7]. The first excited optical transition energy between 1P states is then calculated to be equal to 740 meV ($E = 1243$). The model used in this work is simple, light in computation task and includes geometrical symmetries, which are highly important for physical applications. In addition computed and experimental values of the optical transition energy are in reasonable agreement.

4. Conclusion

The problem of electronic energy levels and wavefunctions in quantum dots was studied with parabolic coordinates. The conventional effective mass Hamiltonian and Schrödinger equation were derived. It was shown that the problem is fully separable for a disc shape in the case of an infinite potential barrier. The solutions are then directly related to the resonance modes of a cavity associated with the Helmholtz equation. Exact solutions for the lens-shaped quantum dots were proposed. This geometry is realistic and is important for numerous applications when orientational symmetries are involved. It is compared to the limiting cases of the quantum well and of the hemispherical quantum dot. It is also applied to self-organized InAs quantum dots grown on InP. Further works will focus on the applications of the analytical solutions found for the lens-shaped quantum dots. Various physical effects such as Stark shifts, excitonic effect, interband or intraband optical absorption will then be studied [18]. The method described in this paper will also be extended to other sets of special coordinates.

References

[1] Grundman M, Bimberg D and Ledentsov N N 1998 *Quantum Dot Heterostructures* (Chichester: Wiley)
[2] Sugawara M 1999 Self-assembled InGaAs/GaAs quantum dots *Semiconductors and Semimetals* vol 60 (Toronto: Academic)
[3] Alferov Zh I 1998 Quantum wires and dots show the way forward *III-Vs Rev.* **11** 47–52
[4] Marzin J Y and Bastard G 1994 *Solid State Commun.* **92** 437
[5] Vasanelli A De, Giorgi M, Ferreira R, Cingolani R and Bastard G 2001 *Physica* E **11** 41
[6] Vasanelli A De, Giorgi M, Ferreira R, Cingolani R, Sakaki H and Bastard G 2001 *Japan. J. Appl. Phys.* **40** 1955
[7] Miska P, Paranthoen C, Even J, Bertru N, Lecorre A and Dehaese O 2002 *J. Phys.: Condens. Matter* **14** 12301
[8] Fossard F, Julien F H, Peronne E, Alexandrou A, Brault J and Gendry M 2001 *Infrared Phys. Technol.* **42** 443
[9] Cantele G, Ninno D and Iadonisi 2000 *J. Phys.: Condens. Matter* **12** 9019
[10] Van den Broeck M and Peeters F M 2001 *Physica* E **11** 345
[11] Wojs A, Hawrylack P, Fafard S and Jacak L 1996 *Phys. Rev.* B **54** 5604
[12] Rodriguez A H, Trallero-Giner C, Ulloa S E and Marin-Antuna J 2001 *Phys. Rev.* B **63** 125319
[13] Arfken G 1966 *Mathematical Method for Physicists* (New York: Academic)
[14] Morse P M and Feshbach H 1953 *Methods of Theoretical Physics* (New York: McGraw-Hill)

[15] Lebedev N N 1972 *Special Functions and Their Applications* (New York: Dover)
[16] Abramovitz M and Stegun I A 1972 *Handbook of Mathematical Functions* (New York: Dover)
[17] Maple V Release 4 (Copyright 1981–1995 by Waterloo Maple Inc.)
[18] Bastard G 1992 *Wave Mechanics Applied to Semiconductor Heterostructures* (Paris: EDP)
[19] Frechengues S, Bertru N, Drouot V, Lambert B, Robinet S, Loualiche S, Lacombe D and Ponchet A 1999 *Appl. Phys. Lett.* **74** 3356
[20] Chuang S L 1995 *Physics of Optoelectronic Devices (Wiley Series in Pure and Applied Optics)* (New York: Wiley)
[21] Paranthoen C, Bertru N, Lambert B, Dehaese O, LeCorre A, Even J, Loualiche S, Lissilour F, Moreau G and Simon J C 2002 *Semicond. Sci. Technol.* **17** L5
[22] Saito H, Nishi K and Sugou S 2001 *Electron. Lett.* **37** 21